Theoretical study of CO adsorption on FexCuy(x+y=3) clusters and reactive activity of their carbonyl complexes

Jianhui Zhang (gszhangjh@126.com)
Yanli Leng
Jing Liu
Huanjiang Wang
Hongmei Mu

Research Article

Keywords: FexCuy (x+y=3), Carbonyl complexes, Density functional theory, Energy gap

Posted Date: July 1st, 2022

DOI: https://doi.org/10.21203/rs.3.rs-1784756/v1

Abstract

In this paper, the adsorption of CO on Fe_xCu_y (x + y = 3) clusters were studied by BPW91 method, all conceivable geometries and electronic states of carbonyl complexes were explored. The results show that bimetallic clusters tend to have higher stepwise CO adsorption energy than corresponding pure clusters, and the adsorption capacity of $FeCu_2(CO)_3$ with CO is substantially larger than that of other carbonyl complexes. Moreover, the frontier molecular orbital theory was used to analyze the effect of the second element in the ligand reactions, which also confirmed that the reactions of CO with bimetallic clusters are easier than that of pure cluster systems. Finally, the energy gaps of HOMO and LUMO were use to explore the reactive activity of carbonyl complexes, it was found that the bimetallic clusters are lower than that of the Fe_3 or Cu_3, and the $Fe_2Cu(CO)_1$ has lower energy gap than that of other carbonyl complexes. This suggests that it may be possible to tune bimetallic cluster to get higher activity carbonyl complexes in the reactions.

1 Introduction

In recent decades, carbonyls and their derivatives have received particular attention due to they play a central role in modern organometallics chemistry [1]. Extensive experimental and theoretical research has been conducted on their synthesis, characterization, and applications, especially for the interaction of metals with metals in these compounds [2–8]. The better known iron and copper carbonyls including mononuclear $Fe(CO)_5$ and $Cu(CO)_3$, dinuclear $Fe_2(CO)_9$ and $Cu_2(CO)_x$ (x = 1–6), trinuclear $Fe_3(CO)_n$ (n = 12, 11, 10, 9), $Cu_3(CO)_7^+$, $Cu_3(CO)_8^+$ and $Cu_3(CO)_9^+$, tetranuclear $Cu_4(CO)_8^+$ [9–13] and so on.

Practically carbonyl complexes consist of not only homonuclear carbonyl but also included heteronuclear carbonyl such as $CuNi(CO)_n^{0/1-}$(n = 1–4), $MNi(CO)_7^-$ (M = V, Nb, Ta), $CuFe(CO)_n^-$ (n = 4–7) and $PbFe(CO)_4^-$ [14–17]. The most unsaturated neutral species apparently have been studied focus on the one carbon monoxide on clusters [18–20]. In a subsequent development, it was shown that the other unsaturated neutral species have special function in synthetic chemistry, just as $Fe(CO)_4$, is isolobal with CH_3^+, which has been used to study both the structure and the bonding in related compounds [21]. Different ligands have been investigated for their interactions with the $Fe(CO)_4$ fragment, and found that the structures of metal-π ligand complexes are remarkable, lending an almost inventive aspect to the organometallic chemistry [22–26].

The purpose of this work is to investigate the adsorption of CO with Fe_xCu_y (x + y = 3) clusters, and compare the reactive activity of carbonyl complexes, using quantum chemistry methods. Therefore, analysis of the structural stability and electronic properties of carbonyl complexes are needed, and understand of the molecular orbital information of species are necessary.

2 Computation Methods

Energies and geometries of the reaction intermediates were calculated using the density functional theory (DFT) method. Exchange-correlation functional consists of the combination of Becke's exchange and Perdew-Wang's correlation functions, which is commonly known as BPW91, within the generalized gradient approximation (GGA) [27–29]. For the present calculations, this functional was combined with the standard 6-311 + G(2d) basis set level[30, 31]. Vibrational frequency calculations were used to characterize all stationary points as either minima (the number of imaginary frequencies NIMAG = 0). All of the DFT computations were carried out with the GAUSSIAN 09 program [32]. The adsorption energies were evaluated from the calculated energies of cluster with adsorbate, E(total), E(Fe_xCu_y) and E(CO) are the energies of $Fe_xCu_y(CO)_n$ cluster, bare Fe_xCu_y cluster and CO molecule, respectively, and using the following equation,

E_{ad} = E(total) - E(Fe_xCu_y) -nE(CO)

3 Results And Discussion

For the metal carbonyl species, only the most stable ones are listed, other optimized geometries and feasible spin multiplicities of the reaction can be obtained from the Supporting Information (Table 1 and Fig S1-S4). Three typical adsorption sites are considered, including top sites, bridge sites and a facet site. The calculated adsorption energies are in agreement with previous experiment and calculations [33, 34].

Table 1
Vibrational frequency, total energy E_T and stepwise CO adsorption energy E_{ad} (kJ/mol) for the $Fe_3(CO)_n$ (n = 0–12).

Species	NIMAG (cm^{-1})	E_T (hartree)	E_{ad} (kJ/mol)	Species	NIMAG (cm^{-1})	E_T (hartree)	E_{ad} (kJ/mol)
$^{11}Fe_3$	73.94	-3791.41	-	$^{5}Fe_3(CO)_7$	12.79	-4585.20	-132.61
$^{9}Fe_3(CO)_1$	46.02	-3904.81	-168.79	$^{3}Fe_3(CO)_8$	30.41	-4698.60	-144.87
$^{9}Fe_3(CO)_2$	18.97	-4018.22	-187.03	$^{1}Fe_3(CO)_9$	22.92	-4811.99	-136.06
$^{9}Fe_3(CO)_3$	20.79	-4131.62	-166.55	$^{1}Fe_3(CO)_{10}$	20.29	-4925.38	-152.60
$^{7}Fe_3(CO)_4$	29.24	-4245.02	-167.80	$^{1}Fe_3(CO)_{11}$	7.79	-5038.75	-66.52
$^{7}Fe_3(CO)_5$	16.39	-4358.42	-152.62	$^{1}Fe_3(CO)_{12}$	32.44	-5152.14	-139.11
$^{5}Fe_3(CO)_6$	31.15	-4471.81	-140.83	CO	2126.25	-113.34	-

3.1 $Fe_3(CO)_n$ (n = 1–12)

The geometrical parameters of the $Fe_3(CO)_n$ (n = 1–12) cluster systems are shown in Fig. 1. Vibrational frequency, total energies E_T, and stepwise CO adsorption energy for the Fe_3 systems are collected in Table 1. According to our study and previous experimental study, the Fe_3 electronic ground state is found to be $^{11}A'$. Table 1 indicates the following, all CO adsorption steps are exothermic, from n = 1–12 for Fe_{13}, the most CO adsorption energy (-187.63 kJ/mol) is found for n = 2 in Fe_3 system. According to research, the most stable geometries tend to occur on one Fe atom to form Fe_2-$Fe(CO)_4$ structure, and then on the second Fe atom until it is saturated, last, up to the last structure $Fe_3(CO)_{12}$. According to the calculated results, the bond length of CO molecule is 1.139 Å. It is clear from Fig. 1, after CO molecules adsorbed on these Fe_3 clusters, the elongation of C-O are extended with the range from 1.3–4.5%, it can think that CO has been activated. The most adsorption energy structure of Fe_3 carbonyl species is $^9Fe_3(CO)_2$ with C_s symmetry, with the most stepwise CO adsorption energy by 187.03 kJ/mol.

3.2 $Fe_2Cu\ (CO)_n$ (n = 1–11)

According to the theoretical calculation, the geometries and parameters of $Fe_2Cu\ (CO)_n$ (n = 1–11) are listed in the Fig. 2 and Table 2. On the basis of the theoretical studies, the ground state of Fe_2Cu is $^8A'$, which is slower than $^6A'$ and $^{10}A''$ by 30.6 and 46.5 kJ/mol, respectively. We first study CO adsorption behavior on both Fe and Cu tops. In contrast, the corresponding adsorption energy value on one Fe side of Fe_2Cu is 188.02 kJ/mol, and the corresponding adsorption energy value on Cu is 121.99 kJ/mol, which is slower than that on Fe atom by 66.03 kJ/mol. The most stable structure of $Fe_2Cu(CO)_n$ (n = 1–11) is found that the CO coordination tend to occur on one Fe atom, later, on the next Fe atom to constitute $Fe(CO)_{1-3}$-Cu-$Fe_2(CO)_4$, last, up to the saturated CO coordination structure. In the carbonyl species, the $^6Fe_2Cu(CO)_1$ with the most E_{ads} by 188.02 kJ/mol, in which, Fe-CO and C-O distances are 1.768 and 1.178 Å, respectively. In $^2Fe_2Cu(CO)_{11}$ complex, the energy of a structure with top site adsorption of CO (doublet state with C_{2v} symmetry) is only 6.71 kJ/mol.

Table 2
Vibrational frequency, total energy E_T and stepwise CO adsorption energy E_{ad} (kJ/mol) for the $Fe_2Cu(CO)_n$ (n = 0–11).

Species	NIMAG (cm^{-1})	E_T (hartree)	E_{ad} (kJ/mol)	Species	NIMAG (cm^{-1})	E_T (hartree)	E_{ad} (kJ/mol)
$^8Fe_2Cu$	73.25	-4168.25	-	$^2Fe_2Cu(CO)_6$	27.45	-4848.66	-146.82
$^6Fe_2Cu(CO)_1$	46.49	-4281.66	-188.02	$^2Fe_2Cu(CO)_7$	7.77	-4962.05	-120.35
$^6Fe_2Cu(CO)_2$	37.55	-4395.06	-163.76	$^2Fe_2Cu(CO)_8$	19.98	-5075.43	-128.27
$^6Fe_2Cu(CO)_3$	31.10	-4508.46	-161.69	$^2Fe_2Cu(CO)_9$	20.30	-5188.81	-114.97
$^4Fe_2Cu(CO)_4$	33.98	-4621.87	-185.43	$^2Fe_2Cu(CO)_{10}$	17.99	-5302.17	-41.33
$^4Fe_2Cu(CO)_5$	22.35	-4735.27	-155.02	$^2Fe_2Cu(CO)_{11}$	15.38	-5415.51	-6.71

3.3 $FeCu_2(CO)_n$ (n = 1–10)

Figure 3 shows the most stable geometries of $FeCu_2(CO)_n$ (n = 1–10). There are several possible ways to evaluate the feature of the $FeCu_2(CO)_n$ (n = 1–10) structures predicted in Table 3. The BPW91 calculations showed that the $FeCu_2$ ground state is the quintet state, which is slower than the triplet and septet states are 20.74 and 61.99 kJ/mol respectively. Analysis of the entire geometries of $FeCu_2(CO)_n$ (n = 1–4) shows that the isomer with CO adsorbed on Fe atom have more stable compared to those with CO combine with Cu atoms. For the $FeCu_2(CO)_6$, it is found that the CO coordination prefer to take place on different Cu atoms, which has lower energy than that of CO coordination on only one Cu atom. In the carbonyl species, the $^1FeCu_2(CO)_4$ has the most E_{ads} by 190.58 kJ/mol.

Table 3
Vibrational frequency, total energy E_T and stepwise CO adsorption energy E_{ad} (kJ/mol) for the $FeCu_2(CO)_n$ (n = 1–10).

Species	NIMAG (cm^{-1})	E_T (hartree)	E_{ad} (kJ/mol)	Species	NIMAG (cm^{-1})	E_T (hartree)	E_{ad} (kJ/mol)
$^5FeCu_2$	110.47	-4545.09	-	$^1FeCu_2(CO)_6$	18.47	-5225.50	-118.18
$^3FeCu_2(CO)_1$	49.61	-4658.51	-189.67	$^1FeCu_2(CO)_7$	15.42	-5338.85	-34.52
$^3FeCu_2(CO)_2$	31.99	-4771.91	-170.23	$^1FeCu_2(CO)_8$	14.07	-5452.20	-44.43
$^1FeCu_2(CO)_3$	33.93	-4885.32	-181.31	$^1FeCu_2(CO)_9$	3.01	-5565.55	-30.41
$^1FeCu_2(CO)_4$	14.87	-4998.73	-190.58	$^1FeCu_2(CO)_{10}$	13.92	-5678.90	-34.58
$^1FeCu_2(CO)_5$	18.27	-5112.11	-122.57				

3.4 $Cu_3(CO)_n$ (n = 1–8)

On the basis of calculation, the Cu_3 ground state is the doublet state, which is lower than the quartet state 166.96 kJ/mol in energy. For $Cu_3(CO)_n$ (n = 1–8), most stable structures and the corresponding geometrical parameters are shown in Fig. 4 and Table 4. In the beginning of the chemisorption process, we study CO adsorption behavior on difference sites of Cu_3 cluster. For the Cu_3CO, the lowest energy state of the complex is a doublet with C_{2v} symmetry, in which CO is adsorbed on the top adsorption site. In the $Cu_3(CO)_2$ complex, a CO molecule is adsorbed on the one of the other two Cu atoms of Cu_2-CuCO, the lowest energy state of the complex is a doublet with C_{2v} symmetry. For the $Cu_3(CO)_5$, the stepwise CO adsorption tend to adsorbed on the top site of last Cu atom of $Cu_3(CO)_4$. In the Cu_3 carbonyl species, the $^2Cu_3(CO)_1$ has the most E_{ads} by 138.93 kJ/mol.

Table 4
Vibrational frequency, total energy E_T and stepwise CO adsorption energy E_{ad} (kJ/mol) for the $Cu_3(CO)_n$ (n = 1–8).

Species	NIMAG (cm^{-1})	E_T (hartree)	E_{ad} (kJ/mol)	Species	NIMAG (cm^{-1})	E_T (hartree)	E_{ad} (kJ/mol)
$^2Cu_3$	105.60	-4921.96	-	$^2Cu_3(CO)_5$	18.21	-5488.83	-68.03
$^2Cu_3(CO)_1$	38.18	-5035.35	-138.93	$^2Cu_3(CO)_6$	13.00	-5602.19	-56.90
$^2Cu_3(CO)_2$	30.30	-5148.72	-100.32	$^2Cu_3(CO)_7$	6.22	-5715.55	-64.98
$^2Cu_3(CO)_3$	15.38	-5262.09	-78.72	$^2Cu_3(CO)_8$	18.19	-5828.90	-33.72
$^2Cu_3(CO)_4$	19.54	-5375.46	-91.61				

3.4 Adsorption energy and molecular orbital properties

The change curve of CO adsorption energy on Fe_xCu_y (x + y = 3) are collected in Fig. 5. Overall, the Cu_3 system has lower CO adsorption capacity on ground state, while the Fe_3 system has a relatively high value of stepwise CO adsorption energy. For the bimetallic clusters, it has been found that the stepwise CO adsorption energy of Fe_2Cu is higher than that on Fe_3 and Cu_3 with n = 1, 4, 5 and 6, that the stepwise CO adsorption energy of $FeCu_2$ is higher than that on Fe_3 and Cu_3 with n = 1, 3 and 4, respectively. For bimetallic systems with $n \geq 7$, the stepwise CO adsorption energy are between Fe_3 and Cu_3. The largest stepwise CO coordination energy (-190.58 kJ· mol^{-1}) is found for $FeCu_2(CO)_4$.

Frontier molecular orbitals of Fe_xCu_y (x + y = 3) cluster systems are collected in Fig. 6 and Supporting Information (Tables S2), where HOMO is the highest occupied molecular orbital of Fe_xCu_y (x + y = 3) carbonyl complexes, ΔE is the energy level difference between the HOMO of carbonyl complexes and the LUMO of CO. In the case of the CO adsorbs on the Fe_xCu_y (x + y = 3) carbonyl complexes, CO molecule obtains electrons from the HOMO of clusters. Based on the study, the molecular reaction can happen only if the ΔE is less than 0.2205 a.u. (579 kJ/mol) [35]. The LUMO energy of free CO is -0.3855 a.u., while the HOMO energies of Fe_xCu_y (x + y = 3) carbonyl complexes are all less than − 0.1650 a.u., it means the transfer of electrons from the HOMO of Fe_xCu_y (x + y = 3) carbonyl complexes to the LUMO of CO is possible. In brief, the smaller of the ΔE is, the easier of the electron transfer to CO would be, also, the reactions of CO with bimetallic carbonyl complexes are easier than pure clusters system, except Fe_3 cluster with first CO molecular.

Frontier molecular orbital theory predicts that the smaller the energy gap (Eg) between the HOMO and LUMO of reactant involved is, the more reactive activity of the molecular would be [36]. The Eg of Fe_xCu_y (x + y = 3) carbonyl complexes are showed in Fig. 7 and Supporting Information (Tables S2). Collectively,

we can obtain that bimetallic carbonyl complexes have lower value of Eg than that of corresponding monometallic carbonyl complexes, except Fe_2Cu and $FeCu_2(CO)_{10}$. This study also gets a good relation of contacting the values of the adsorption energy with Eg of carbonyl complexes, observing in this case that the smaller Eg is, on the contrary, the greater adsorption energy is. The lowest Eg of all carbonyl species is $^2Fe_2Cu(CO)_8$ with the value of 2.63 kJ/mol.

4 Conclusions

The ligand addition reactions of the CO adsorption over the clusters of Fe_xCu_y (x + y = 3) have been studied by BPW91 method. For monometallic clusters, all CO coordination steps are exothermic, the largest CO coordination energy (-187.03 and − 138.93 kJ/mol) are found for n = 1 in Fe_3 and Cu_3 system. For bimetallic clusters, the largest CO coordination energies are found − 188.02 and − 190.58 kJ/mol for $Fe_2Cu(CO)_1$ and $FeCu_2(CO)_4$, respectively. The most stable molecules are approaching CO coordinate with Fe atoms, then, on the Cu atoms. Moreover, the FMOs were used to analyze the Eg between the HOMO and LUMO of the Fe_xCu_y (x + y = 3) carbonyl complexes, and found that the bimetallic carbonyl complexes have smaller Eg than corresponding pure metallic. Our findings show that the bimetallic clusters can have higher adsorption energy, and the decrease of Eg implied that carbonyl complexes might show the higher activity than the pure clusters.

Declarations

Acknowledgement

This study was supported by the Scientific Research Foundation of Guizhou Minzu University (GZMUZK[2021]YB11) and (GZMUZK[2019]YB31), Guizhou Provincial Science and Technology Projects ([2019]1158), Guizhou Provincial Science and Technology Projects for Youth Talents (KY[2018]149), Higher Education Innovation Foundation of Gansu Province (2021A-254).

References

1. Zhou M, Andrews L, Bauschlicher CW (2001) Spectroscopic and theoretical investigations of vibrational frequencies in binary unsaturated transition-metal carbonyl cations, neutrals, and anions. Chem Rev 101:1931–1962
2. King AD, King DB, Yang DB (1980) Homogeneous catalysis of the water gas shift reaction using iron pentacarbonyl. J Am Chem Soc 102:1028–1032
3. Allan M, Lacko M, Papp P, Matejčík Š, M Zlatar, Il Fabrikant, J Kočišek, J Fedor (2018) Dissociative electron attachment and electronic excitation in $Fe(CO)_5$ Phys Chem Chem Phys 20:11692–11701
4. Huang C, Huang L, Li G, Xie Y, King RB, Schaefer HF (2021) Fluorine migration from carbon to iron and fluorine-iron dative bonds in octafluorocyclohexadiene iron carbonyl chemistry. Organometallics 40:397–407

5. Liu Z, Xie H, Qin Z, Fan H, Tang Z (2014) Structural evolution of homoleptic heterodinuclear copper-nickel carbonyl anions revealed using photoelectron velocity-map imaging. Inorg Chem 53:10909–10916
6. Liu Z, Bai Y, Li Y, He J, Lin Q, Zhang F, Wu HS, Jia J (2020) Triply carbonyl-bridged $Ni_2(CO)_5$ featuring triple three-center two-electron Ni-C-Ni bonds instead of Ni ≡ Ni triple bond. Inorg Chem 59:15365–15374
7. Buchwalter P, Rose J, Braunstein P (2015) Multimetallic catalysis based on heterometallic complexes and clusters. Chem Rev 115:28–126
8. Liu N, Guo L, Cao Z, Li W, Zheng X, Shi Y, Guo J, Xi Y (2016) Mechanisms of the water-gas shift reaction catalyzed by ruthenium carbonyl complexes, J Phys Chem A 120:2408–2419
9. Li Q, Li YN, Wang T, Wang SG, Huo CF, Li YW, Wang JG, Jiao HJ (2013) Electronic structures and energies of $Fe_2(CO)_n$ (n = 0–9). Chemphyschem 14: 1573–1576
10. Jang JH, Lee JG, Lee H, Xie Y, Schaefer HF (1998) Molecular structures and vibrational frequencies of iron carbonyls: $Fe(CO)_5$, $Fe_2(CO)_9$, and $Fe_3(CO)_{12}$. J Phys Chem A 102: 5298–5304
11. Li Q, Liu Y, Xie Y, King RB, Rd SH (2001) Binuclear homoleptic copper carbonyls $Cu_2(CO)_x$ (x = 1–6): remarkable structures contrasting metal-metal multiple bonding with low-dimensional copper bonding manifolds. Inorg Chem 40:5842–5850
12. Cui J, Zhou X, Wang G, Chi C, Liu Z, Zhou M (2013) Infrared photodissociation spectroscopy of mass selected homoleptic copper carbonyl cluster cations in the gas phase. J Phys Chem A 117:7810–7817
13. Dewar J, Jones HO (1907) On a new iron carbonyl, and on the action of light and of heat on the iron carbonyls. Proc R Soc 79:66–80
14. Liu Z, Xie H, Qin Z, Fan H, Tang Z (2014) Structural evolution of homoleptic heterodinuclear copper-nickel carbonyl anions revealed using photoelectron velocity-map imaging. Inorg Chem 53:10909–10916
15. Zhang J, Li G, Yuan Q, Zou J, Yang D, Zheng H, Wang C, Yang J, Jing Q, Liu Y, Fan H, Xie H (2020) Photoelectron velocity map imaging spectroscopic and theoretical study of heteronuclear $MNi(CO)_7^-$ (M = V, Nb, Ta). J Phys Chem A 124:2264–2269
16. Zhang N, Luo M, Chi C, Wang G, Cui J, Zhou M (2015) Infrared photodissociation spectroscopy of mass-selected heteronuclear iron-copper carbonyl cluster anions in the gas phase. J Phys Chem A 119:4142–4150
17. Liu Z, Zou J, Qin Z, Xie H, Fan H, Tang Z (2016) Photoelectron velocity map imaging spectroscopy of lead tetracarbonyl-iron anion $PbFe(CO)_4^-$. J Phys Chem A 120:3533–3538
18. Lanzani G, Nasibulin AG, Laasonen K, Kauppinen EI (2009) CO dissociation and CO + O reactions on a nanosized iron cluster. Nano Res 2: 660–670
19. Sousa PF, Andriani KF, Silva J (2021) Ab initio Investigation of the role of the d-states occupation on the adsorption properties of H_2, CO, CH_4 and CH_3 OH on the Fe_{13}, Co_{13}, Ni_{13} and Cu_{13} clusters. Phys

Chem Chem Phys 23:8739–8751

20. Padilla-Campos L (2008) Theoretical study of the adsorption of carbon monoxide on small copper clusters. J Mol Struc-Theochem 851:15–21
21. Cunden LS, Linck RG (2011) $Fe(CO)_4$ and related compounds as isolobal fragments. Inorg Chem 50:4428–4436
22. Macdonald CLB, Cowley AH (1999) A theoretical study of free and $Fe(CO)_4$-complexed borylenes (boranediyls) and heavier congeners.J Am Chem Soc 121:12113–12126
23. Su J, Li XW, Crittendon RC, Campana CF, Robinson GH (1997) Experimental confirmation of an iron-gallium multiple bond: synthesis, structure, and bonding of a ferrogallyne. Organometallics 16:4511–4513
24. Zandiyeh Z, Ghiasi R, Jamaat P R (2020) Computational rationalization of the interaction of $Fe(CO)_4$ and substituted benzyne ligands. J Struct Chem 61:197–206
25. Goumans TPM, Ehlers AW, van Hemert M C, Rosa A, Baerends EJ, Lammertsma K (2003) Photodissociation of the phosphine-substituted transition metal carbonyl complexes $Cr(CO)_5L$ and $Fe(CO)_4L$: A theoretical study. J Am Chem Soc 125:3558–3567
26. Ghiasi R, Peikari A (2017) Solvent Effects on Stability, electronic structure, and ^{14}N NQR parameters of $Fe(CO)_4$py isomers. J Appl Spectrosc 84:148–155
27. Becke AD (1988) Density-functional exchange-energy approximation with correct asymptotic behavior. Phys Rev A 38:3098–3100
28. Perdew JP, Wang Y (1992) Accurate and simple analytic representation of the electron-gas correlation energy. Phys Rev B 45:13244–13249
29. White JA, Bird DM (1994) Implementation of gradient-corrected exchange-correlation potentials in car-parrinello total-energy calculations. Phys Rev B 50:4954–4957
30. McLean AD, Chandler GS (1980) Contracted gaussian-basis sets for molecular calculations 1.2nd row atoms, Z = 11–18. J Chem Phys 72:5639–5648
31. Krishnan R, Binkley JS, Seeger R, Pople JA (1980) Self-consistent molecular orbital methods XX A basis set for correlated wave function. J Chem Phys 72:650–654
32. Frisch MJ, Trucks GW, Schlegel HB, Scuseria GE, Robb MA, Cheeseman JR, Scalmani G, Barone V, Mennucci B, Petersson GA, Nakatsuji H, Caricato M, Li X, Hratchian HP, Izmaylov AF, Bloino J, Zheng G, Sonnenberg JL, Hada M, Ehara M, Toyota K, Fukuda R, Hasegawa J, Ishida M, Nakajima T, Honda Y, Kitao O, Nakai H, Vreven T, Montgomery JA, Peralta JrJE, Ogliaro F, Bearpark M, Heyd JJ, Brothers E, Kudin KN, Staroverov VN, Kobayashi R, Normand J, Raghavachari K, Rendell A, Burant JC, Iyengar SS, Tomasi J, Cossi M, Rega N, Millam JM, Klene M, Knox JE, Cross JB, Bakken B, Adamo C, Jaramillo J, Gomperts R, Stratmann RE, Yazyev O, Austin AJ, Cammi R, Pomelli C, Ochterski JW, Martin RL, Morokuma K, Zakrzewski VG, Voth GA, Salvador P, Dannenberg JJ, Dapprich S, Daniels AD, Farkas O, Foresman JB, Ortiz JV, Cioslowski J, Fox DJ GAUSSIAN 09 (Revision E01), Gaussian, Inc, Wallingford CT, 2013

33. Wang H, Xie Y, King RB, Schaefer HF (2006) Remarkable aspects of unsaturation in trinuclear metal carbonyl clusters: the triiron species $Fe_3(CO)_n$ (n = 12, 11, 10, 9). J Am Chem Soc 128:11376–11384
34. Pakiari AH, Mousavi M (2011) Influence of copper substitution on the interaction of ethylene over iron clusters: a theoretical study. J Phys Chem A 115:11796–11809
35. Wei ZD, Yan AZ, Feng YC, Feng YC, Li L, Sun CX, Shao ZG, Shen PK (2007) Study of hydrogen volution reaction on Ni-P amorphousalloy in the light of experimental and quantum chemistry. Electrochem Commun 9:2709–2715
36. Greenwood HH (1952) A molecular orbital theory of reactivity in aromatic hydrocarbons. J Chem Phys 20:1653–1654

Figures

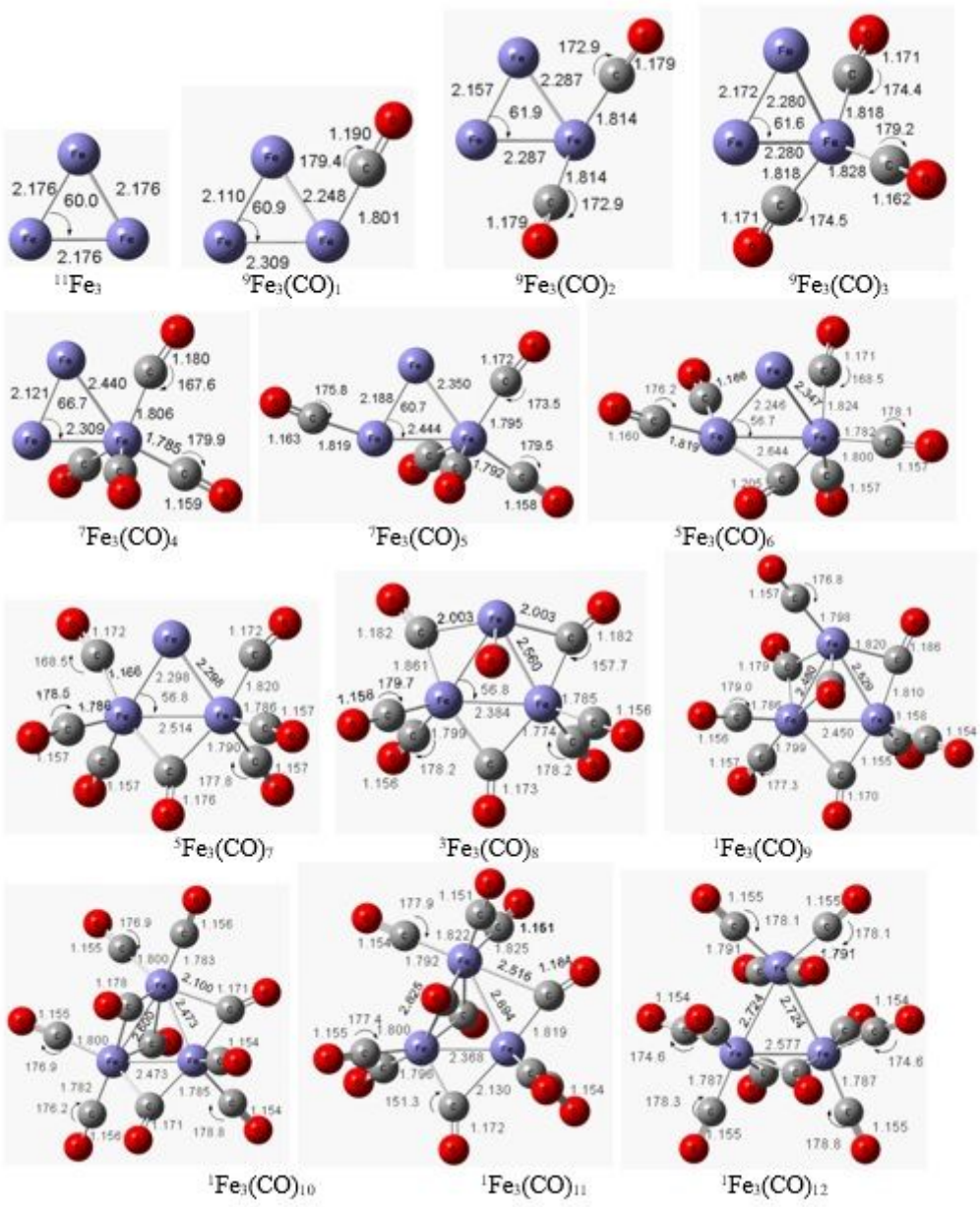

Figure 1

Geometries of the $Fe_3(CO)_n$ (n=1-12) on the ground electronic state at the bpw91/6-311+G(2d) level (bond length in angstrom and bond angle in degree)

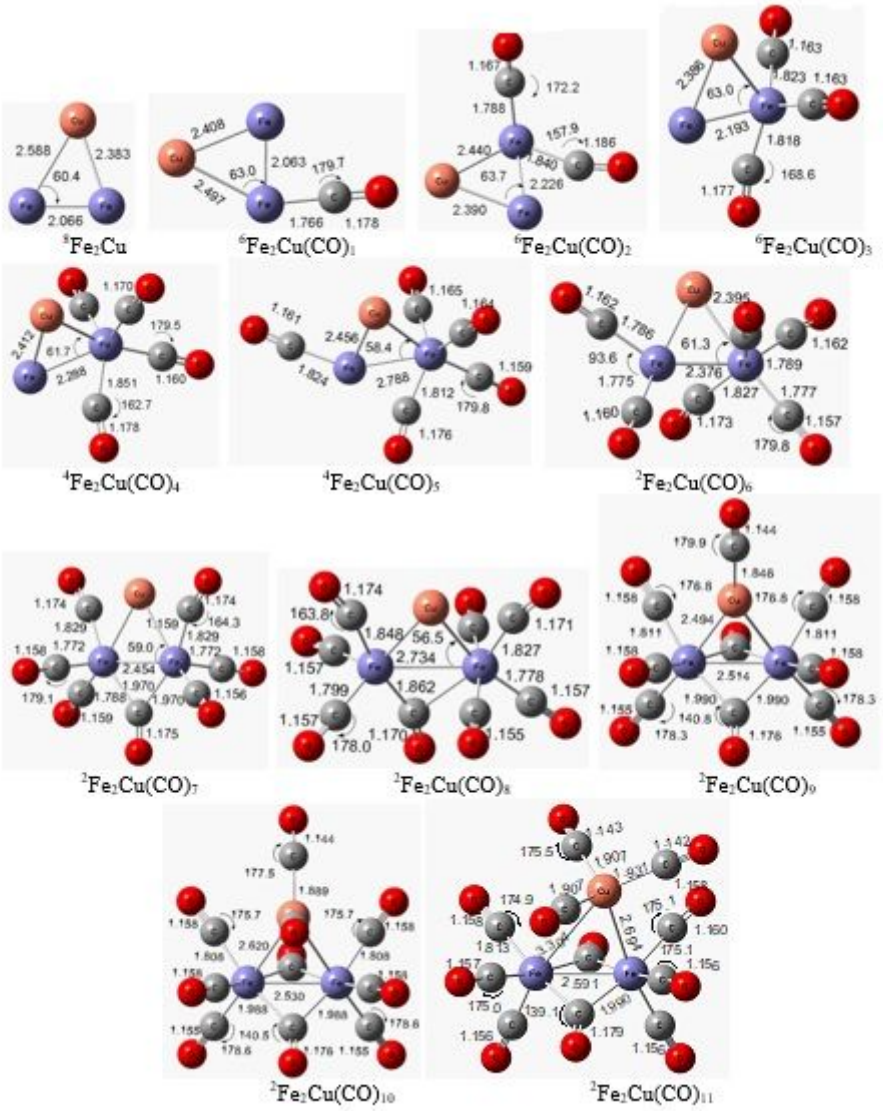

Figure 2

Geometries of the $Fe_2Cu(CO)_n$ (n=1-11) on the ground electronic state at the bpw91/6-311+G(2d) level (bond length in angstrom and bond angle in degree)

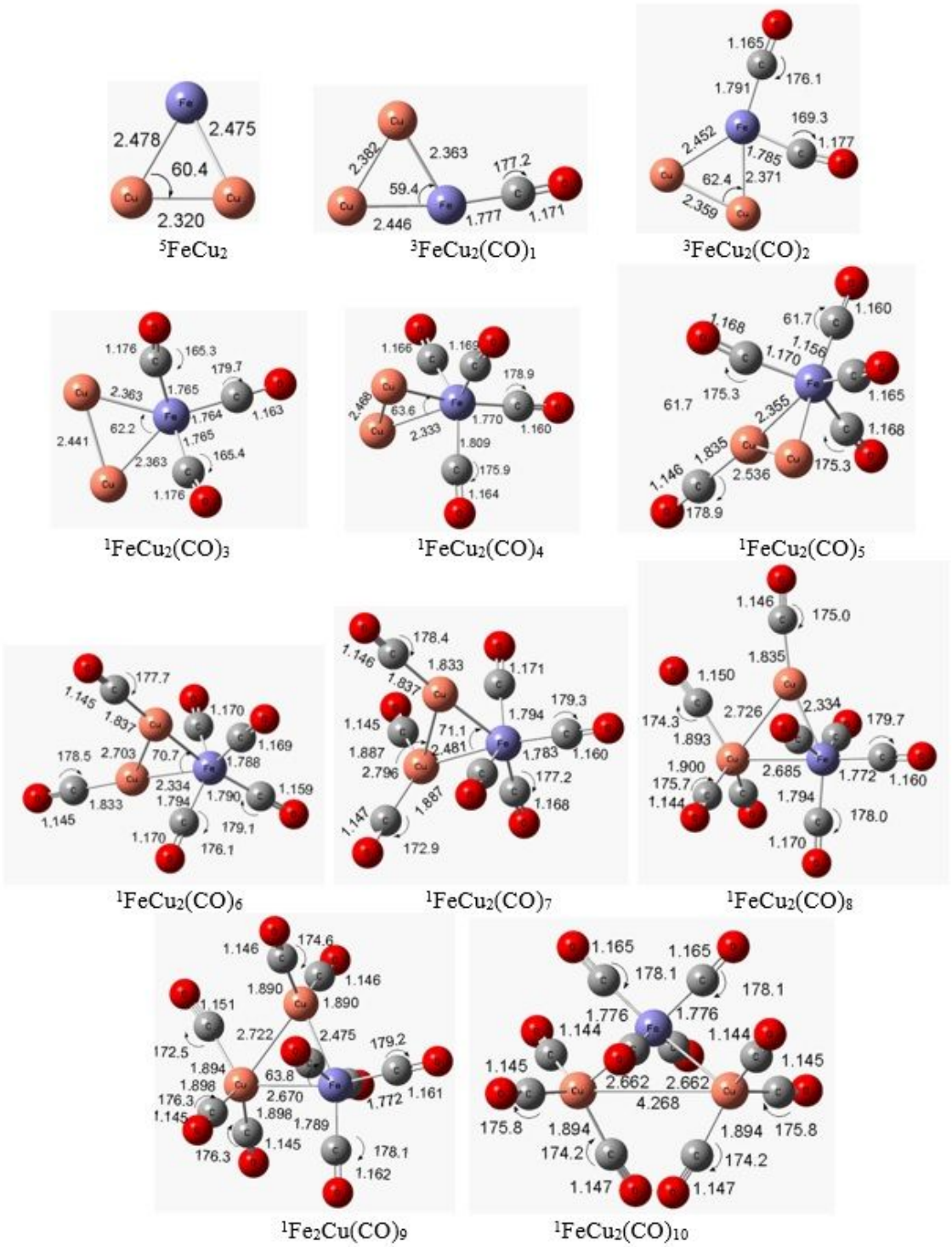

Figure 3

Geometries of the $FeCu_2(CO)_n$ (n=1-10) on the ground electronic state at the bpw91/6-311+G(2d) level (bond length in angstrom and bond angle in degree)

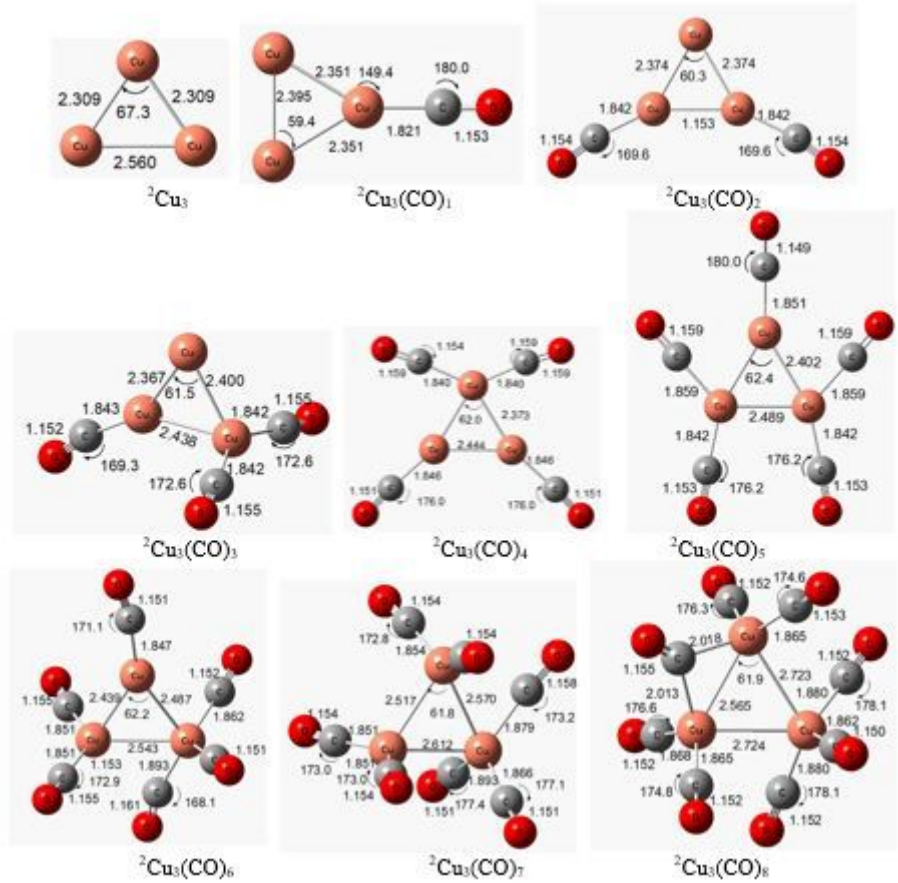

Figure 4

Geometries of the $Cu_3(CO)_n$(n=1-8) on the ground electronic state at the bpw91/6-311+G(2d) level (bond length in angstrom and bond angle in degree)

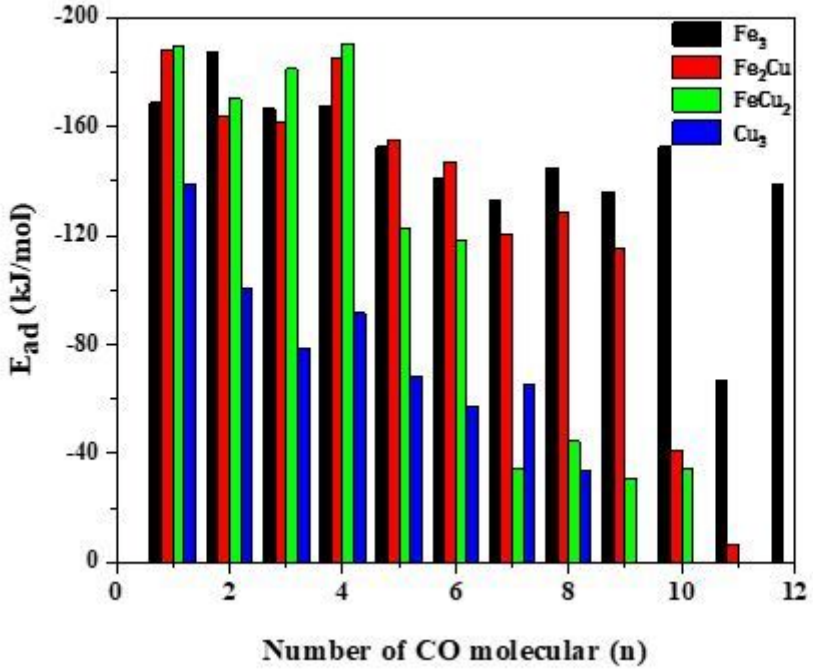

Figure 5

Stepwise CO adsorption energy of CO on the Fe_xCu_y (x+y=13) clusters

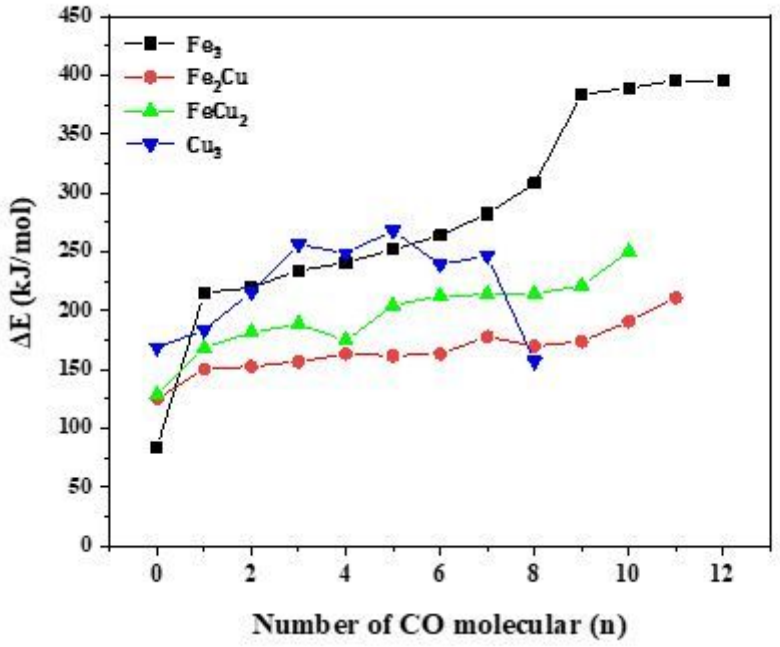

Figure 6

The ΔE of HOMO of Fe_xCu_y (x+y=13) carbonyl complexes with LUMO of CO

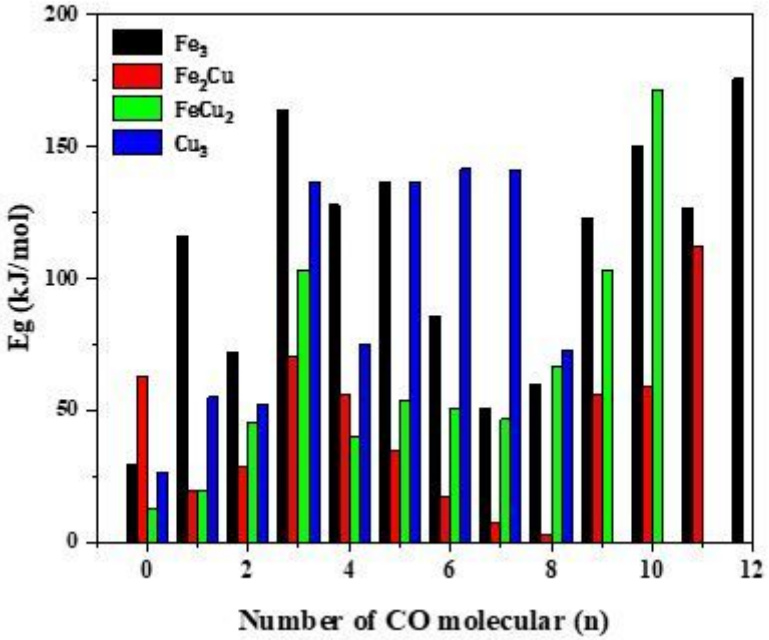

Figure 7

The Eg of HOMO with LUMO of Fe_xCu_y (x+y=13) carbonyl complexes

Supplementary Files

This is a list of supplementary files associated with this preprint. Click to download.

- SupportingInformation.doc